

See discussions, stats, and author profiles for this publication at: <https://www.researchgate.net/publication/7757056>

# Electrochemical Sensing Based on Redox Mediation at Carbon Nanotubes

ARTICLE *in* ANALYTICAL CHEMISTRY · AUGUST 2005

Impact Factor: 5.64 · DOI: 10.1021/ac050059u · Source: PubMed

---

CITATIONS

184

---

READS

57

## 2 AUTHORS:



**Maogen Zhang**

University of Texas at San Antonio

22 PUBLICATIONS 1,247 CITATIONS

SEE PROFILE



**Waldemar Gorski**

University of Texas at San Antonio

55 PUBLICATIONS 2,098 CITATIONS

SEE PROFILE

# Electrochemical Sensing Based on Redox Mediation at Carbon Nanotubes

Maogen Zhang and Waldemar Gorski\*

The Department of Chemistry, University of Texas at San Antonio, San Antonio, Texas 78249

An electrochemical sensing platform was developed based on the integration of redox mediators and carbon nanotubes (CNT) in a polymeric matrix. To demonstrate the concept, a redox mediator Azure dye (AZU) was covalently attached to polysaccharide chains of chitosan (CHIT) and interspersed with CNT to form composite films for the amperometric determination of  $\beta$ -nicotinamide adenine dinucleotide (NADH). The incorporation of CNT into CHIT-AZU matrix facilitated the AZU-mediated electrooxidation of NADH. In particular, CNT decreased the overpotential for the mediated process by an extra 0.30 V and amplified the NADH current by  $\sim 35$  times (at  $-0.10$  V) while reducing the response time from  $\sim 70$  s for CHIT-AZU to  $\sim 5$  s for CHIT-AZU/CNT films. These effects were discussed in terms of the AZU/CNT synergy, which improved charge propagation through the CHIT-AZU/CNT matrix. The concept of CNT-facilitated redox mediation in polymeric matrixes has a potential to be of general interest for expediting redox processes in electrochemical devices such as sensors, biosensors, and biological fuel cells and reactors.

The integration of redox mediators (RM) and carbon nanotubes (CNT) in polymeric matrixes for the development of electrochemical sensors has not been explored thus far. At first, the concept may even appear to be counterintuitive because both RM and CNT provide similar benefits to electrochemical sensing in terms of lowering the overpotential of electrode processes.<sup>1–9</sup> Thus, the introduction of RM into the CNT-based sensors could be perceived as a redundant and complicating factor in the sensor design.<sup>7–10</sup> Regardless of these perceptions, however, we show here that the integration of RM and CNT in a polymeric matrix

can provide a remarkable synergistic augmentation of sensor performance. To demonstrate the concept, the phenothiazine derivatives Azure dyes (AZU) and CNT were co-immobilized in the matrix of a biopolymer chitosan (CHIT) and tested as a sensing platform for the amperometric determination of  $\beta$ -nicotinamide adenine dinucleotide (NADH).

The determination of NADH is important because the  $\text{NAD}^+/\text{NADH}$  couple is the cofactor system for a large number of dehydrogenase enzymes ( $>300$ ) and a component of biomarker systems. Electrochemical sensors for NADH are particularly attractive because they can provide high sensitivity and low detection limit, and they can be miniaturized. However, the selectivity and stability of electrochemical determination of NADH have been often inadequate because of a large overpotential ( $>1$  V) for the direct oxidation of NADH at conventional electrodes. Recently, CNT-based electrodes have been shown to reduce significantly the NADH overpotential,<sup>2,9,11–15</sup> although the extent of such a reduction has not been enough to ensure selective determination of NADH. A traditional approach to lowering the oxidation potential of NADH has relied on the use of redox mediators with low formal potentials.<sup>3</sup> Phenothiazine derivatives such as AZU dyes are attractive in this respect because they are chemically reactive and display negative formal potentials (vs  $\text{Ag}/\text{AgCl}/3\text{ M NaCl}$ ) at neutral pH. The NADH detectors have been developed based on the AZU dyes that have been either adsorbed,<sup>16</sup> electropolymerized,<sup>17,18</sup> or covalently attached<sup>19</sup> to the electrode surface. However, such modified surfaces displayed rather limited stability and redox mediation capacity toward NADH. For example, the oxidation of NADH at such surfaces still required the application of positive potentials, which diminished the selectivity of NADH determination. As presented below, these and other problems of redox-mediated determination of NADH can be overcome by integrating AZU dyes with CNT in hydrophilic films of CHIT on the surface of glassy carbon electrodes.

\* Corresponding author: (fax) 210-458-7428; (e-mail) waldemar.gorski@utsa.edu.

- (1) Davis, J. J.; Coles, R. J.; Hill, H. A. O. *J. Electroanal. Chem.* **1997**, *440*, 279–282.
- (2) Wang, J.; Deo, R. P.; Poulin, P.; Mangey, M. *J. Am. Chem. Soc.* **2003**, *125*, 14706–14707.
- (3) Gorton, L.; Dominguez, E. *Rev. Mol. Biotechnol.* **2002**, *82*, 371–392.
- (4) Gao, M.; Dai, L.; Wallace, G. G. *Synth. Met.* **2003**, *137*, 1393–1394.
- (5) Nugent, J. M.; Santhanam, S. V.; Rubio, A.; Ajayan, P. M. *Nano Lett* **2001**, *1*, 87–91.
- (6) Wu, K.; Fei, J.; Hu, S. *Anal. Biochem.* **2003**, *318*, 100–106.
- (7) Rubianes, M. D.; Rivas, G. A. *Electrochem. Commun.* **2003**, *5*, 689–694.
- (8) Luong, J. H. T.; Hrapovic, S.; Wang, D.; Bensebaa, F.; Simard, B. *Electroanalysis* **2004**, *16*, 132–139.
- (9) Zhang, M.; Smith, A.; Gorski, W. *Anal. Chem.* **2004**, *76*, 5045–5050.
- (10) Antiochia, R.; Lavagnini, I.; Pastore, P.; Magno, F. *Bioelectrochemistry* **2004**, *64*, 157–163.

- (11) Musameh, M.; Wang, J.; Merkoci, A.; Lin, Y. *Electrochem. Commun.* **2002**, *4*, 743–746.
- (12) Wang, J.; Musameh, M. *Anal. Chem.* **2003**, *75*, 2075–2079.
- (13) Liu, P.; Yuan, Z.; Hu, J.; Lu, J. *Proc.-Electrochem. Soc.* **2003**, *13*, 346–356.
- (14) Moore, R. R.; Banks, C. E.; Compton, R. G. *Anal. Chem.* **2004**, *76*, 2677–2682.
- (15) Chen, J.; Bao, J.; Cai, C.; Lu, T. *Anal. Chim. Acta* **2004**, *516*, 29–34.
- (16) Chi, Q.-J.; Dong, S.-J. *J. Mol. Catal. A: Chem.* **1996**, *105*, 193–201.
- (17) Cai, C.-X.; Xue, K.-H. *J. Electroanal. Chem.* **1997**, *427*, 147–153.
- (18) Gao, Q.; Wang, W.; Ma, Y.; Yang, X. *Talanta* **2004**, *62*, 477–482.
- (19) Ohtani, M.; Kuwabata, S.; Yoneyama, H. *J. Electroanal. Chem.* **1997**, *422*, 45–54.

The present paper focuses on (1) covalent attachment of AZU molecules to CHIT chains, (2) electrochemical responses of CHIT-AZU, CHIT/CNT, and CHIT-AZU/CNT films to NADH, and (3) synergistic effects in the CHIT-AZU/CNT system. The analytical performance of the CHIT-AZU/CNT film electrodes as amperometric sensors for NADH is presented as well.

## EXPERIMENTAL SECTION

**Reagents.** Multiwalled CNT (20–50-nm diameter,  $\sim 1\text{--}5\text{ }\mu\text{m}$  length,  $\sim 95\%$  nominal purity) were purchased from Nanolab (Brighton, MA). They were used as received because further purification with hot strong acids and heating at high temperatures<sup>20</sup> had virtually no effect on the electrooxidation of NADH. CHIT (MW  $\sim 1 \times 10^6$ ;  $\sim 80\%$  deacetylation), sodium cyanoborohydride, glutaric dialdehyde, Azure A, and Azure C dyes (AZU), and NADH were purchased from Sigma-Aldrich. Other chemicals such as  $\text{NaH}_2\text{PO}_4 \cdot \text{H}_2\text{O}$ ,  $\text{Na}_2\text{HPO}_4$ , HCl, and NaOH were from Fisher. All solutions were prepared using deionized water that was purified with a Barnstead NANOpure cartridge system. Solutions of chemically modified chitosan were dialyzed using dialysis membrane tubings (Fisher,  $1.2\text{--}1.4 \times 10^4$  MWCO).

**Electrochemical Measurements.** A CHI 832B workstation (CH Instruments, Inc.) was used to collect electrochemical data. Experiments were performed at room temperature ( $20 \pm 1\text{ }^\circ\text{C}$ ) in a conventional three-electrode system with 3.0-mm-diameter glassy carbon (GC) disk working electrode (Bioanalytical Systems, Inc.), a platinum wire as the auxiliary electrode, and a Ag/AgCl/3 M NaCl (BAS) reference electrode. All of the potentials are reported versus this reference. Prior to use, the GC electrodes were wet polished on an Alpha A polishing cloth (Mark V Lab) with successively smaller particles (0.3- and  $0.05\text{-}\mu\text{m}$  diameter) of alumina. The slurry that accumulated on the electrode surface was removed by ultrasonication for 30 s in deionized water and methanol.

The phosphate buffer solutions (0.05 M, pH 7.40) served as a background electrolyte. The experiments were repeated at least three times, and the means of measurements are presented with the standard deviations or relative standard deviations.

**Chitosan Solutions.** The stock solutions of 0.10 wt % CHIT were prepared by dissolving chitosan flakes in hot ( $80\text{--}90\text{ }^\circ\text{C}$ ) 0.10 M HCl. Solutions were cooled to room temperature, and their pH was adjusted to 5.0 using the NaOH solutions. Such CHIT solutions were subsequently filtered using a  $0.45\text{-}\mu\text{m}$  Millex-HA syringe filter unit (Millipore) and stored in a refrigerator ( $4\text{ }^\circ\text{C}$ ) when not in use. All chitosan solutions were colorless.

**Preparation of Film Electrodes.** The preparation of films was optimized in order to maximize their signal-to-noise ratio for the determination of NADH. The most sensitive CHIT-AZU/CNT films were prepared using 0.040 vol % CHIT-AZU solutions that contained  $0.50\text{ mg mL}^{-1}$  dispersed by 15-min sonication. The  $10\text{-}\mu\text{L}$  aliquots of such CHIT-AZU/CNT solutions were mixed with  $30\text{ }\mu\text{L}$  of water and cast on the surface of GC electrodes. The evaporation of water for 1–2 h resulted in thin CHIT-AZU/CNT surface films that contained  $5\text{ }\mu\text{g}$  of CNT. The films were circular with  $\sim 4\text{-mm}$  diameter ( $\sim 0.12\text{ cm}^2$ ), which completely covered the  $3.0\text{-mm}$ -diameter ( $0.071\text{ cm}^2$ ) GC disk. Other films

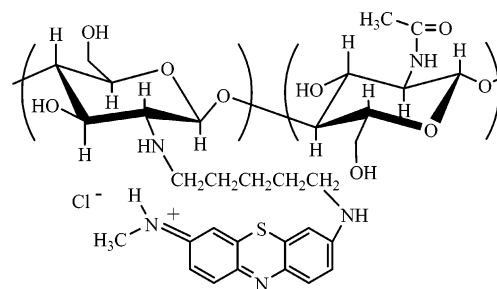


**Figure 1.** Structure of chitosan with covalently attached redox mediator Azure C. The Schiff bases in the CHIT-AZU product were reduced using sodium cyanoborohydride.

such as CHIT, CHIT-AZU, and CHIT/CNT were prepared in the analogous manner by casting relevant solutions on the surface of GC electrodes.

Prior to their first use, the film electrodes were soaked in buffer solutions (100 mL) for 4 h and washed repeatedly with deionized water to remove loosely bound material. When not in use, the film electrodes were stored in deionized water at room temperature.

## RESULTS AND DISCUSSION

In the preliminary studies, two redox-active dyes Azure A and Azure C were investigated as redox mediators. While both molecules are similar (Supporting Information) and display a comparable redox behavior, the films with Azure C generated  $\sim 60\%$  more current in the presence of NADH in a solution. Therefore, detailed investigations were continued with Azure C. Throughout the paper, the abbreviation AZU relates to Azure C.

**Modification of Chitosan with Azure.** The covalent attachment of AZU molecules to CHIT chains relied on the formation of Schiff bases by reacting amino groups of AZU and CHIT with bifunctional tether molecules of glutaric dialdehyde. In step I, an aqueous solution of 0.10 wt % CHIT was mixed with an excess of glutaric dialdehyde and allowed to react for 48 h at room temperature. To react only one aldehyde group of dialdehyde with amino groups of CHIT, a high molar ratio of glutaric dialdehyde to CHIT glucosamine units (200:1) was used.<sup>21</sup> The unreacted dialdehyde was removed from the solution by dialyzing it for 12 h against three 1-L batches of HCl solution (pH 4.5). The progress of species removal was monitored by using UV–visible spectrophotometry. In step II, the solution of CHIT–glutaric dialdehyde was reacted with the AZU dye for 12 h at  $80\text{ }^\circ\text{C}$ . The amount of AZU used was equivalent to the content of glucosamine units of CHIT in the solution. Again, the dialysis was used to remove unreacted AZU molecules from the reaction mixture. Finally, the Schiff bases in the CHIT-AZU product (Figure 1) were reduced to more stable secondary amines using sodium cyanoborohydride.

The results of synthesis were corroborated by infrared (IR) spectroscopy of films I and II that were prepared by evaporating water from dialyzed reaction mixtures after steps I and II, respectively. Prior to spectroscopic measurements, the films were extensively soaked in pH 7.40 phosphate buffer solutions and washed with deionized water to remove any loosely bound material. Figure 2 shows IR spectra of films I and II as well as a reference spectrum of CHIT film (trace a). The spectrum of a

(20) Dillon, A. C.; Gennett, T.; Jones, K. M.; Alleman, J. L.; Parilla, P. A.; Heben, M. J. *Adv. Mater.* **1999**, *11*, 1354–1348.

(21) Wei, X.; Cruz, J.; Gorski, W. *Anal. Chem.* **2002**, *74*, 5039–5046.

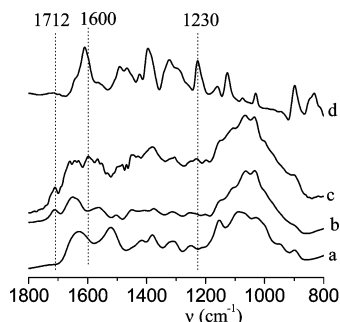


**Figure 2.** Infrared spectra of (a) CHIT, (b) CHIT–glutaric dialdehyde (film I), (c) CHIT–glutaric dialdehyde–AZU (film II), and (d) AZU films.

film I (trace b) displayed the absorption band at  $1712\text{ cm}^{-1}$ , which was characteristic for an aldehyde group. This confirmed that molecules of glutaric dialdehyde were attached to CHIT with one end, leaving a free aldehyde group on the other end. Film II (trace c) continued to display the absorption band at  $1712\text{ cm}^{-1}$ , which indicated that not all free aldehyde groups were used up in the reaction with AZU. This observation is important for the future biosensor development because the unreacted aldehyde groups can be used for the covalent immobilization of enzymes in such materials. The  $1712\text{-cm}^{-1}$  band disappeared from the spectrum of film II only after the reduction with sodium cyanoborohydride (Supporting Information). The spectrum of the film II displayed new bands at  $1600$  and  $1230\text{ cm}^{-1}$  (trace c), which were due to absorption by aromatic rings of AZU (trace d).

The immobilization of AZU molecules on CHIT chains was further supported by UV–visible spectrophotometry. The latter revealed that dialyzed solution II, in contrast to dialyzed solution I, displayed the absorption peak at  $623\text{ nm}$ , which was close to the absorption peak of free AZU ( $617\text{ nm}$ ) dissolved in water (Supporting Information).

The content of AZU in the CHIT-AZU product was determined by subtracting the micromoles of unreacted AZU from the total number of micromoles of AZU used for the reaction. In a typical procedure, a  $4.0\text{-mL}$  aliquot of  $0.10\text{ wt } \%$  CHIT–glutaraldehyde (solution I) was reacted with  $20.0\text{ }\mu\text{mol}$  of AZU for  $12\text{ h}$  at  $80\text{ }^{\circ}\text{C}$  and then dialyzed for  $12\text{ h}$  against three  $1\text{-L}$  batches of HCl solution ( $\text{pH } 4.5$ ). Such a procedure resulted in a removal of all of the free AZU dye from the CHIT-AZU solution. This was confirmed by the lack of the dye absorption bands in the electronic spectrum of the third dialysate solution. The UV–visible spectrophotometry of the first two dialysate solutions revealed that they contained a total of  $16.8\text{ }\mu\text{mol}$  of AZU, which indicated that  $3.2\text{ }\mu\text{mol}$  ( $= 20.0 - 16.8$ ) of AZU was immobilized on CHIT chains. Since the aliquot contained  $\sim 20\text{ }\mu\text{mol}$  of CHIT glucosamine units ( $\text{FW} = 161\text{ g mol}^{-1}$ ), the molar ratio of AZU to monomer units of glucosamine in the CHIT-AZU product was  $\sim 1:6$ . This ratio indicated that most of the free aldehyde groups in the product remained unreacted, which was consistent with the IR data (Figure 2, trace c).

**Voltammetric and Amperometric Analysis of the CHIT-AZU/CNT System.** In the initial control experiments, cyclic voltammograms of free AZU dissolved in a solution were recorded at a bare glassy electrode. Figure 3 (trace a1) shows that voltammograms contained a pair of current peaks due to the redox of AZU at a midpoint potential of  $-0.21\text{ V}$ . The addition of NADH to the AZU solution resulted in the appearance of a new broad

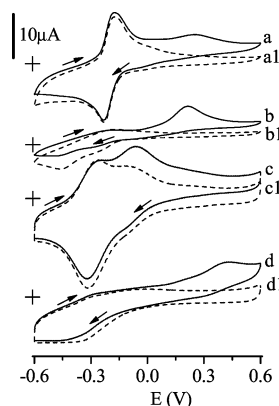


**Figure 3.** Cyclic voltammograms recorded in  $1.0\text{ mM}$  NADH solutions at (a) bare GC electrode, and (b) CHIT-AZU, (c) CHIT-AZU/CNT, and (d) CHIT/CNT films that were cast on the surface of GC electrodes. Voltammograms a and a1 were recorded in NADH +  $0.25\text{ mM}$  AZU and  $0.25\text{ mM}$  AZU solutions, respectively. Background voltammograms for film electrodes b1, c1, and d1 were obtained in  $\text{pH } 7.40$  phosphate buffer. Scan rate,  $50\text{ mV s}^{-1}$ .

anodic peak at  $+0.25\text{ V}$  on the cyclic voltammogram (trace a). Since the direct oxidation of NADH at the glassy carbon takes place at potentials more positive than  $+0.5\text{ V}$ , this new peak was ascribed to the AZU-mediated oxidation of NADH. The mediation involved the reduction of AZU by NADH and reoxidation of the reduced AZU molecules at the electrode surface. The latter process generated the current peak, which will be referred to as the mediation peak. The large difference between the potentials of the mediation peak ( $+0.25\text{ V}$ ) and the original anodic peak of AZU ( $-0.18\text{ V}$ ) indicated that the reaction between AZU and NADH in the solution was slow on the time scale of the experiment.

Cyclic voltammetry was subsequently used to determine the role of individual components in the CHIT-AZU/CNT system. To this end, the voltammetric and amperometric response of CHIT, CHIT-AZU, and CHIT/CNT films to NADH was recorded and compared to that of a CHIT-AZU/CNT film. The CHIT film proved to be a structural matrix that was electrochemically silent in the potential window used in this work (not shown). The cyclic voltammogram of a CHIT-AZU film contained a pair of poorly defined and small peaks of AZU at a midpoint potential of  $-0.21\text{ V}$  (Figure 3, trace b1) and an extra cathodic peak at  $-0.45\text{ V}$ , which probably reflected heterogeneity of AZU redox sites in the film. In the presence of NADH in the solution, the cathodic peaks of AZU decreased while a new anodic peak appeared at  $+0.22\text{ V}$  (trace b), which was consistent with the pattern of redox mediation. The shift of the mediation peak from  $+0.25\text{ V}$  for the bare electrode (trace a) to  $+0.22\text{ V}$  for the film electrode (trace b) suggested some improvement in the efficiency of redox mediation in the CHIT-AZU film.

The introduction of CNT into CHIT-AZU films influenced the films' voltammetric characteristics in a way that indicated the presence of synergistic effects in the CHIT-AZU/CNT system. First, CNT improved the redox behavior of AZU immobilized in CHIT-AZU/CNT films. This was indicated by the appearance of distinct current peaks at  $-0.28\text{ V}$  (trace c1). These peaks were less separated and  $\sim 13 \pm 1$  times larger than those yielded by CHIT-AZU films at  $-0.21\text{ V}$  (trace b1). One could argue that the increase in current peaks was due to an extra surface area



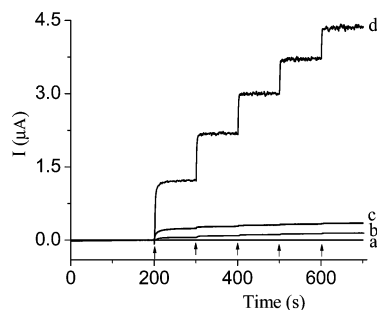


**Figure 4.** Current traces ( $E = -0.10$  V) recorded at (a) CHIT, (b) CHIT-AZU, (c) CHIT/CNT, and (d) CHIT-AZU/CNT film electrodes. Steps represent the response of the films to additions of 0.10 mM NADH (arrows) in a stirred solution of phosphate buffer, pH 7.40.

provided by the CNT for the redox of AZU immobilized on chitosan chains. However, this does not explain the enhanced electron transfer to NADH (vide infra). The control voltammetric experiments with a freely diffusing model probe  $\text{Fe}(\text{CN})_6^{3-}$  showed that current peaks of the probe were only  $\sim 1.5 \pm 0.1$  times larger at CHIT-AZU/CNT than at CHIT-AZU film electrodes. This small increase in the probe's peaks correlated with a comparably small increase, by  $\sim 1.7 \pm 0.2$  times, in the geometric surface area of the CHIT-AZU/CNT film ( $\sim 0.12 \text{ cm}^2$ ) over that of the GC disk ( $0.071 \text{ cm}^2$ ). Apparently, the probe's current reflected only the apparent surface area of the CHIT-AZU/CNT film rather than the total surface area of individual CNT. This is consistent with the overlapping of the diffusion layers formed at closely spaced CNT in the film during the time necessary to record cyclic voltammograms.

Second, the introduction of CNT into CHIT-AZU films facilitated the AZU-mediated oxidation of NADH. This was indicated by the shift in the mediated peak toward less positive potentials by 0.30 V, i.e., from +0.22 (trace b) to  $-0.08$  V (trace c). Such a decrease in the peak potential could not be ascribed to the direct oxidation of NADH at CNT because the direct oxidation yielded a current peak at a much more positive potential (+0.41 V, trace d). The 0.30-V shift in the mediation peak could not be explained by the shift in the original AZU peaks, which moved only by 0.07 V, i.e., from  $-0.21$  V (trace b1) to  $-0.28$  V (trace c1). The control experiment showed that the pertinent shift in the  $\text{Fe}(\text{CN})_6^{3-/4-}$  peaks was only  $\sim 0.02$  V (not shown).

The positive synergy in the CHIT-AZU/CNT system could also be demonstrated by the amperometric data. Figure 4 shows current traces recorded at film electrodes that were polarized at  $-0.10$  V in a stirred solution, which was spiked with NADH stock solution. The CHIT film yielded no current response to NADH, which confirmed that CHIT played the role of an electrochemically silent structural matrix (trace a). At CHIT-AZU films, a detectable but very small current response to NADH on the order of  $\sim 10^{-8}$  A was observed (trace b). The direct oxidation of NADH at CNT of CHIT/CNT films was also ineffective at  $-0.10$  V (trace c). Only the integrated film of CHIT-AZU/CNT generated a high and dynamic current output due to AZU-mediated oxidation of NADH (trace d). Based on data in Figure 4, the synergistic amplification of amperometric detection of NADH at a CHIT-AZU/CNT film electrode can be expressed by the condition  $I_{(\text{AZU}+\text{CNT})} \gg I_{\text{AZU}} + I_{\text{CNT}}$ , where  $I_{(\text{AZU}+\text{CNT})}$  is the current due to AZU-mediated oxidation

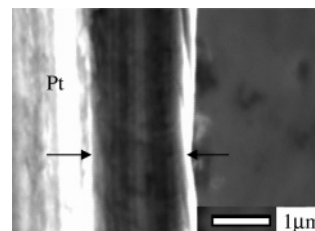


**Figure 5.** Scanning electron micrograph of a cross section of CHIT-AZU/CNT film cast on the surface of a platinum foil.

of NADH at the integrated CHIT-AZU/CNT film (trace d) and  $I_{\text{AZU}}$  and  $I_{\text{CNT}}$  are the NADH currents recorded at individual films CHIT-AZU (trace b) and CHIT/CNT (trace c), respectively.

To explain the above effects, the following synergy hypothesis was formulated. The CNT-induced enhancement in the redox behavior of AZU and AZU-mediated oxidation of NADH could be ascribed to improved electronic and ionic transport capacity of the CHIT-AZU/CNT films. One could presume that the interpenetration of the electron-conducting network of CNT and ion-conducting matrix of CHIT-AZU allowed for the electrooxidation of AZU molecules distant from the GC surface. This shortened the distances over which the electron had to be propagated via hopping between the immobilized AZU molecules. The improved charge propagation through the CHIT-AZU/CNT matrix facilitated the reaction between the AZU and NADH, which resulted in the shift of the mediation peak closer to the original AZU peak (Figure 3, trace c). This, in turn, led to the increase in the  $I_{(\text{AZU}+\text{CNT})}$  current at  $-0.10$  V (Figure 4, trace d).

The following observations supported the hypothesis. First, scanning electron micrographs (Figure 5) showed that the cross section of a CHIT-AZU/CNT composite film resembled the cross section of the Pt foil, which supported the film. This suggested that CNT were distributed throughout the film rather than clustered in distinct regions. One can relate this to the ability of chitosan solutions to form stable colloidal suspensions of CNT.<sup>9</sup> Apparently, upon evaporation of water from suspensions of CNT in chitosan solutions, the CHIT-CNT interactions promoted the uniform dispersion of CNT in the CHIT matrix.

Second, amperometric response of the films to NADH (Figure 6) demonstrated that introduction of CNT into the CHIT-AZU matrix amplified the current at  $-0.10$  V by  $\sim 35$  times while reducing the response time ( $t_{90\%}$ ) from  $\sim 70$  s for CHIT-AZU to  $\sim 5$  s for CHIT-AZU/CNT films. The shorter response time was indicative of faster charge transport in films with CNT.

Third, the influence of CNT on the voltammetry of a CHIT-AZU film included the decrease in the separation of AZU peaks by  $\sim 40$  mV and, as indicated above, their shift by  $\sim 70$  mV toward lower overpotentials (Figure 3, traces b1 and c1). Such voltammetric changes were another indicator of more efficient electron transfer and ion transport in CHIT-AZU/CNT than in CHIT-AZU films. The lowering of AZU overpotential, despite the accompanying increase in the current density, could also suggest a degree of electrocatalytic properties of CNT toward the redox of AZU.

Fourth, in another control experiment, the CNT were substituted with a comparable amount of graphite particles (Gp, 1–2- $\mu\text{m}$  diameter). However, in the presence of NADH in the solution, such a CHIT-AZU/Gp film electrodes yielded currents that were

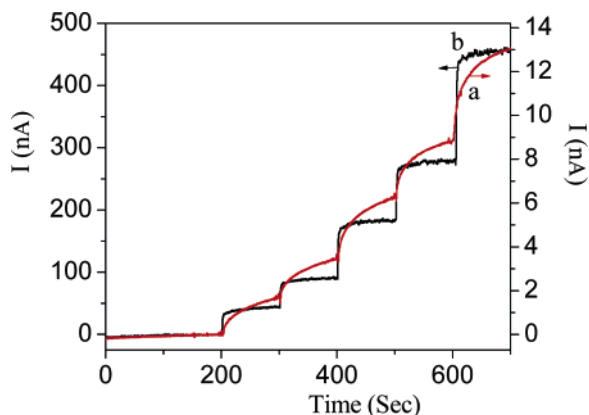


**Figure 6.** Amperometric traces ( $E = -0.10$  V) illustrating a difference in response times of (a) CHIT-AZU and (b) CHIT-AZU/CNT films to additions of 5, 5, 10, 10, and 20  $\mu\text{M}$  NADH to a stirred solution of phosphate buffer, pH 7.40. Note the difference in current scales.

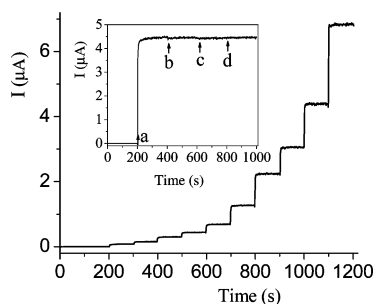


**Figure 7.** Amperometric response ( $E = -0.10$  V) of a CHIT-AZU/CNT film electrode to additions of NADH aliquots (5.0  $\mu\text{M}$ –1.0 mM) into a stirred solution of phosphate buffer, pH 7.40. Inset: Current trace recorded at the CHIT-AZU/CNT film ( $E = -0.10$  V) in a stirred buffer solution (pH 7.40) that was spiked with (a) 0.50 mM NADH, (b) 0.10 mM uric acid, (c) 0.10 mM acetaminophen, and (d) 0.10 mM ascorbic acid.

comparable to those generated by the particle-free CHIT-AZU films. This correlated with the inability of chitosan solutions to form colloidal suspensions of graphite particles. It appears that weak interactions between graphite particles and CHIT chains precluded their intimate mixing in order to improve charge transport in such films.

**Analytical Performance of CHIT-AZU/CNT Film Electrodes.** Figure 7 presents an amperometric trace recorded at a CHIT-AZU/CNT film electrode that was polarized at  $-0.10$  V in a stirred buffer solution, which was spiked with aliquots of NADH stock solution. The current flowing through the film electrode increased in a stepwise manner after each addition of NADH. The analysis of the current steps revealed the following values for the analytical figures of merit. The CHIT-AZU/CNT electrodes displayed high sensitivity ( $10.3 \text{ mA M}^{-1}$ ), low detection limit (0.5  $\mu\text{M}$  NADH at  $S/N = 3$ ), fast response time ( $\sim 5$  s), wide dynamic range (0.5  $\mu\text{M}$ –10 mM), and linear range from 0.5 to 350  $\mu\text{M}$  NADH ( $R^2 = 0.998$ ). While comparable values have been reported for other amperometric NADH sensors, their assemblage in one sensor is an exception rather than a rule.<sup>3,16–19,22</sup> For example, recently developed boron-doped diamond film electrodes have displayed an excellent detection limit for NADH (0.01  $\mu\text{M}$ ).<sup>23</sup>

(22) Prieto-Simon, B.; Fabregas, E. *Biosens. Bioelectron.* **2004**, *19*, 1131–1138.

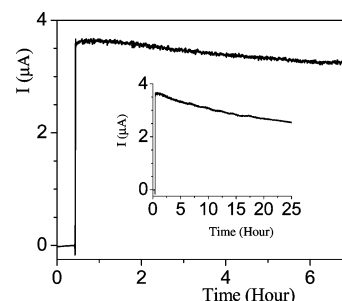


**Figure 8.** Current traces illustrating the operational stability of a CHIT-AZU/CNT film electrode under continuous polarization ( $E = -0.10$  V) and continuous exposure to a stirred solution of 0.50 mM NADH (pH 7.40).

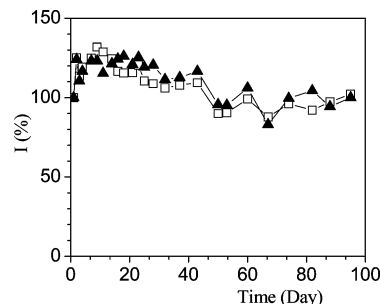


**Figure 9.** Shelf life of three CHIT-AZU/CNT film electrodes that were stored in deionized water when not in use. The data points represent film's current response to 0.50 mM NADH (pH 7.40) measured for 5 min at  $-0.10$  V on a given day. The response was normalized with respect to that on day 1.

However, their linear range has been rather limited (0.01–0.50  $\mu\text{M}$ ) and detection potential was high ( $+0.60$  V). Recently developed nonelectrochemical (fluorescence) assays for NADH displayed detection limits as low as 0.02–0.1  $\mu\text{M}$ ; however, the linearity range extended only to below 10  $\mu\text{M}$ .<sup>24–26</sup>

Perhaps the most attractive feature of the CHIT-AZU/CNT system as the NADH detector is its selectivity and stability. The low detection potential of the CHIT-AZU/CNT films ( $-0.10$  V) eliminated interferences from other redox-active molecules such as ascorbic acid, uric acid, and acetaminophen (Figure 7, inset), which are typically present in biological samples. The CHIT-AZU/CNT film electrodes also displayed useful operational and long-term stability. Typically, they retained  $\sim 80\%$  of the initial signal even after 24 h of continuous polarization ( $-0.10$  V) and continuous exposure to elevated levels of NADH (Figure 8). This demonstrated a good resistance of the CHIT-AZU/CNT film to fouling, which is a common to the oxidation of NADH at other solid electrodes.<sup>3,9</sup> Figure 9 shows that shelf life of the CHIT-AZU/CNT films was at least 100 days.

## CONCLUSIONS

A rather unexpected outcome of the integration of a redox-active matrix of CHIT-AZU with CNT was a degree of the

(23) Rao, T. N.; Yagi, I.; Miwa, T.; Tryk, D. A.; Fujishima, A. *Anal. Chem.* **1999**, *71*, 2506–2511.

(24) Wise, D. D.; Shear, J. B. *Anal. Biochem.* **2004**, *326*, 225–233.

(25) Wang, Z.; Yeung, E. S. J. *Chromatogr., B* **1997**, *695*, 59–65.

(26) Markuszewski, M. J.; Britz-McKibbin, P.; Shigeru, T.; Matsuda, K.; Nishioka, T. *J. Chromatogr., A* **2003**, *989*, 293–301.

AZU/CNT synergy that led to improved charge transport in the matrix. The interpenetration of CHIT-AZU and CNT networks resulted in the amplification of AZU-mediated oxidation of NADH beyond that expected from the extra surface area provided by CNT for the redox of AZU. The analytical benefits of such a synergy included a sensitive, selective, and reliable amperometric quantification of NADH. The CHIT-AZU/CNT composites have a potential to provide the operational access to a large group of NAD<sup>+</sup>-dependent dehydrogenase enzymes for designing a variety of electrochemical devices.

#### **ACKNOWLEDGMENT**

The NIH/MBRS/SCORE Grant GM 08194 supported this work.

#### **SUPPORTING INFORMATION AVAILABLE**

Additional information as noted in text. This material is available free of charge via the Internet at <http://pubs.acs.org>.

Received for review January 11, 2005. Accepted April 12, 2005.

AC050059U